

Effect of zirconium addition on formation of CoSi_2 thin films

FANXIONG CHENG*, CHUANHAI JIANG, XIANPING DONG, HAIFENG WU, JIANSHENG WU

Key Laboratory for High Temperature Materials and Tests of Ministry of Education, School of Materials Science and Engineering, Shanghai Jiao Tong University, Shanghai, People's Republic of China, 200030

E-mail: Chengfanxiong@sjtu.edu.cn

Published online: 25 August 2005

CoSi_2 thin films were prepared by annealing the amorphous Co-Si thin films. Zr was added into the amorphous thin film in order to investigate its effect on formation of CoSi_2 thin film. It was found that Zr increased the crystallization nucleation barrier and accelerated the complete transformation of CoSi to CoSi_2 . © 2005 Springer Science + Business Media, Inc.

1. Introduction

CoSi_2 thin films have been widely researched for ohmic contacts, low resistivity gates and local buried interconnects in ultra-large-scale integrated device (ULSI) [1]. Epitaxial CoSi_2 thin films can be fabricated on Si (100) by solid phase reaction [2, 3] and polycrystalline CoSi_2 thin films can be prepared by annealing of co-deposited thin films of cobalt and silicon [4–6]. Generally the thin films prepared by co-deposition, such as co-sputtering and co-evaporation, are amorphous and need be annealed to form crystalline CoSi_2 . CoSi_2 or Co_2Si was the first crystallized phase when the amorphous $\text{Co}_{0.33}\text{Si}_{0.67}$ film was annealed [4, 5]. However, our work reported [7] that CoSi appeared firstly from the amorphous $\text{Co}_{0.33}\text{Si}_{0.67}$ thin films prepared by radio frequency magnetron sputtering using CoSi_2 alloy target. In this paper the crystallization of the amorphous $\text{Co}_{0.33}\text{Si}_{0.67}$ thin films was further investigated by DSC (differential scanning calorimeter).

Acceleration of the transformation of CoSi to CoSi_2 is helpful to prepare CoSi_2 thin films. Research [8] showed that the addition of Fe, Ge and some other elements into CoSi_2 thin film retarded the transformation of CoSi to CoSi_2 . This was attributed to the fact that these elements were soluble in CoSi and insoluble in CoSi_2 , which caused a change in mixing entropy and resulted in an increased nucleation barrier of CoSi_2 . For the elements that were insoluble in CoSi and soluble in CoSi_2 , such as Ni, the opposite effect was observed. However, for Zr, Ti and the other elements that were insoluble in both cobalt monoxide and disilicide, no change of the CoSi_2 nucleation temperature would be expected. Some reports [9, 10] showed that Zr or Ti addition increased the thermal stability of CoSi. Generally it can be concluded that the full transformation of CoSi to CoSi_2 would be delayed. However, our result

showed that Zr addition increased the thermal stability of CoSi but accelerated the complete transformation of CoSi to CoSi_2 . And also, the effect of Zr addition on the crystallization was studied in this paper.

2. Experiments

The CoSi_2 alloy target was prepared as described in reference [7] and the 5% (atomic ratio) Zirconium was added into the alloy to prepare the three-element alloys target. Energy dispersive X-ray analysis (EDXA) was used to analyze the contents of the target and the results showed that the target had good uniformity.

The thin films with the content similar to $\text{Co}_{0.33}\text{Si}_{0.67}$ or $\text{Co}_{31.7}\text{Si}_{63.3}\text{Zr}_5$ were deposited on the Si (100) and single crystal KCl substrates in a CEVP-1000C magnetron sputtering system. The silicon substrates were cleaned and stripped of the native oxide in diluted HF solution, and immediately inserted into the deposition chamber. The base pressure in the sputtering system was better than 1×10^{-4} Pa, and the deposition was carried out in 1 Pa high pure argon. The substrates remained below 60°C. For the two types of thin films, the deposition rate and total film thickness were about 9 nm min^{-1} and 1.0 μm , respectively. The sputtering power was 450 W. The deposited films on the KCl were dissolved in deionized water and then collected for DSC. XRD (X-ray diffraction) was carried out to investigate structure change of the thin films.

3. Results

EDXA shows that the elements in the as-deposited film distribute uniformly and the composition is similar to the corresponding targets. At the same time, XRD shows that the as-deposited thin films are all

*Author to whom all correspondence should be addressed.

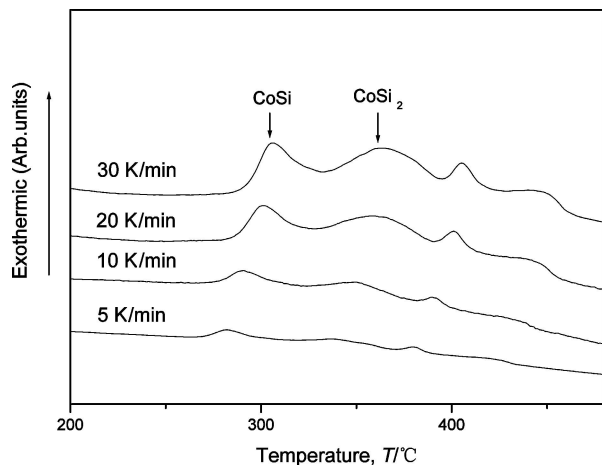


Figure 1. Continuous heating DSC curves of amorphous $\text{Co}_{0.33}\text{Si}_{0.67}$ thin film at 5, 10, 20 and 30°C/min, respectively.

amorphous. The crystallization of these amorphous thin films is now investigated.

3.1. Crystallization

3.1.1. Crystallization of the amorphous $\text{Co}_{0.33}\text{Si}_{0.67}$ film

Typical constant-heating-rate DSC traces of the amorphous $\text{Co}_{0.33}\text{Si}_{0.67}$ film at different heating rates are shown in Fig. 1. In each scan four exothermic peaks were observed. The crystallization peak temperatures were increased as the heating rate was increased. Corresponding XRD patterns of the thin film annealed at different temperatures are plotted in Fig. 2. It was shown that CoSi precipitated at about 250°C, which corresponded to the first exothermic peak. CoSi₂ appeared when the thin film was annealed at about 300°C, which corresponded to the second exothermic peak in Fig. 1. When the thin film was annealed at higher temperatures, no new phase appeared. When CoSi and CoSi₂ formed, the excessive silicon atoms diffused into the un-crystallized amorphous thin film, which elevated the crystallization temperature of the un-crystallized amorphous thin film. Therefore the last two exothermic peaks correspond to the further precipitation of CoSi and CoSi₂, which will be explained further in the following text. The mechanism of CoSi first formation was discussed in our previous paper [7]. According to Kissinger's method, the activation energy of CoSi and CoSi₂ formation can be determined. The Kissinger's equation can be expressed as

$$\ln(\beta/T_p^2) = -E/RT_p + \text{constant}$$

Where T_p is the peak temperature of the crystallization, β is the heating rate, E is the activation energy and R the gas constant. The line plots of $\ln(\beta/T_p^2)$ and $1/T_p$ are illustrated in Fig. 3. The crystallization activation energy can be calculated from the line slope. E_1 and E_2 , determined as 179 kJ/mol and 209.5 kJ/mol, are the apparent activation energies of the formation of CoSi and CoSi₂ in the $\text{Co}_{0.33}\text{Si}_{0.67}$ film, respectively. E_3 , equal to

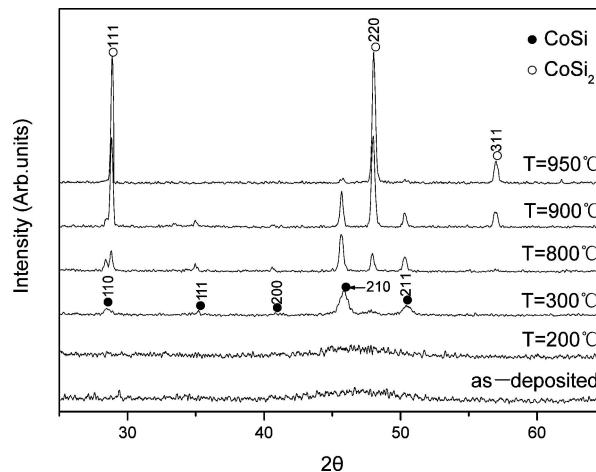


Figure 2. XRD patterns of amorphous $\text{Co}_{0.33}\text{Si}_{0.67}$ thin film annealed at different temperatures.

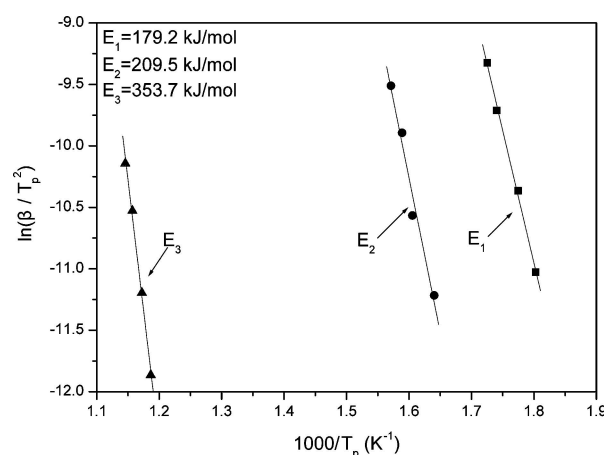


Figure 3. Plot of $\ln(\beta/T_p^2)$ vs. $1/T_p$ for the crystallization of CoSi, CoSi₂ in the amorphous $\text{Co}_{0.33}\text{Si}_{0.67}$ and $\text{Co}_{31.7}\text{Si}_{63.3}\text{Zr}_5$ thin films.

353.7 kJ/mol, is the crystallization activation energy of the Zr-containing film.

3.1.2. Crystallization of the amorphous $\text{Co}_{31.7}\text{Si}_{63.3}\text{Zr}_5$ film

DSC Curves of the amorphous $\text{Co}_{31.7}\text{Si}_{63.3}\text{Zr}_5$ film are depicted in Fig. 4. In each scan only one exothermic peak was observed, which was apparently different from that of the amorphous $\text{Co}_{0.33}\text{Si}_{0.67}$ film. The Zr-containing thin film started to crystallize at an apparently higher temperature and the crystallization activation energy of the amorphous film is determined as 353.7 kJ/mol by Kissinger's method, which is much higher than those of CoSi and CoSi₂ formation in the amorphous $\text{Co}_{0.33}\text{Si}_{0.67}$. XRD patterns of the Zr-containing film annealed at different temperatures are given in Fig. 5. The crystallization of the amorphous film began at about 550°C and CoSi and CoSi₂ formed simultaneously. When the $\text{Co}_{31.7}\text{Si}_{63.3}\text{Zr}_5$ film was annealed above 750°C, there are apparent ZrSi₂ (131) peak in the XRD pattern.

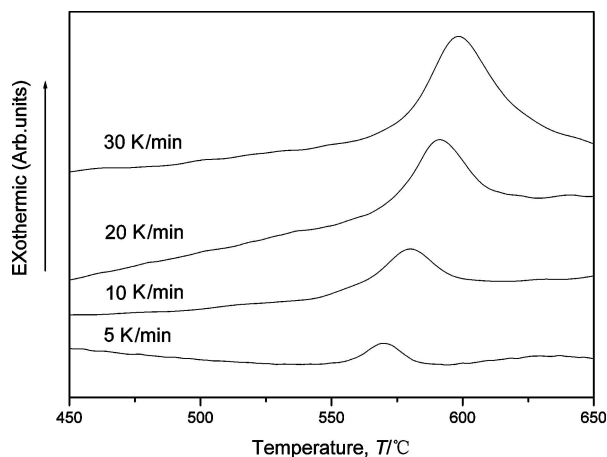


Figure 4 Continuous heating DSC curves of amorphous $\text{Co}_{31.7}\text{Si}_{63.3}\text{Zr}_5$ thin film at 5, 10, 20 and 30°C/min, respectively.

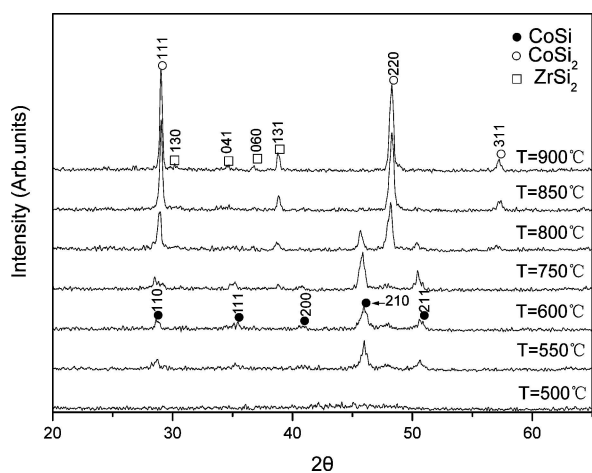


Figure 5 XRD patterns of amorphous $\text{Co}_{31.7}\text{Si}_{63.3}\text{Zr}_5$ thin film annealed at different temperatures.

3.2. Transformation of CoSi to CoSi_2

The direct comparison method [11] was adopted to calculate the phase content of CoSi_2 . Fig. 6 reflects the volume fraction of CoSi_2 when $\text{Co}_{0.33}\text{Si}_{0.67}$ film is annealed at different temperatures. It was shown that CoSi kept stable under 550°C. It also shows the volume fraction of CoSi_2 in the $\text{Co}_{31.7}\text{Si}_{63.3}\text{Zr}_5$ film at different temperatures. During these calculations, ZrSi_2 is not taken into account. It was shown that CoSi and CoSi_2 kept stable until 750°C. However, CoSi quickly transformed into CoSi_2 when the Zr-contained thin film was heated above 800°C. CoSi_2 was fully obtained at 850°C in the $\text{Co}_{31.7}\text{Si}_{63.3}\text{Zr}_5$ film while CoSi was completely transformed at 950°C in the $\text{Co}_{0.33}\text{Si}_{0.67}$ film.

4. Discussions

4.1. Effect of Zr on crystallization of the amorphous thin films

Zr is insoluble in both cobalt monoxide and disilicide [8]. Zr distributes uniformly in the amorphous thin films from the result of EDXA. Crystallization of amorphous alloys begins with the nucleation of a crystal phase. When cobalt monoxide and disilicide nucleate, zirconium atoms must be expelled out of the nucleation area. Because Zr atoms are much

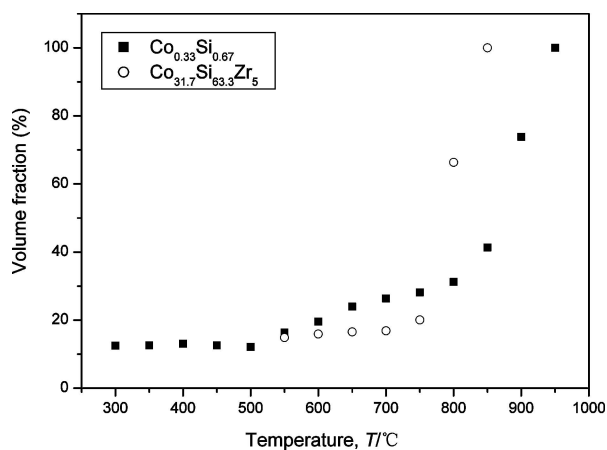


Figure 6 CoSi_2 volume fraction in the $\text{Co}_{0.33}\text{Si}_{0.67}$ and $\text{Co}_{31.7}\text{Si}_{63.3}\text{Zr}_5$ thin film annealed at different temperatures.

larger than Co and Si atoms, they diffuse difficultly and the barrier for crystallization is elevated. Therefore crystallization temperature and crystallization activation energy of the Zr-containing thin film are both increased.

In the amorphous thin film without Zr, the barrier for CoSi nucleation is lower than that for CoSi_2 nucleation, so CoSi and CoSi_2 precipitate in sequence. The crystallization temperature of amorphous materials of Co-Si system was related with the element content. When CoSi_2 formed from amorphous $\text{Co}_{0.2}\text{Si}_{0.8}$ thin film, excessive Si emigrated into the un-crystallized amorphous film and then increased the crystallization temperatures. So the full crystallization of the film need elevate the annealing temperature [4]. In our experiments, CoSi formed firstly from the thin film with the contents as CoSi_2 and the excessive Si emigrated into the amorphous part and then caused the change of Si content in the thin film. Excessive Si increased the crystallization temperature of un-crystallized thin film and then there are two exothermic peaks for the crystallization of CoSi. According to the same principle, there are two exothermic peaks for the crystallization of CoSi_2 . So there are four apparent crystallization exothermic peaks in the DSC curves. In the Zr-containing amorphous film, Co and Si diffuse much more easily than Zr and the barrier of nucleation is mainly decided by Zr diffusion. CoSi and CoSi_2 formed simultaneously when the nucleation barrier was surpassed at about 550°C. During the crystallization, the change of Si content happened but the barrier of crystallization was decided by the diffusion of Zr, so there is one exothermic peak in each DSC scan. It means the Zr-containing thin film can crystallize fully as soon as the crystallization barrier is surpassed.

4.2. Effect of Zr on the transformation of CoSi to CoSi_2

During the crystallization, Zr atoms must be expelled out from the nucleation area. Because Zr is insoluble in CoSi and CoSi_2 , Zr atoms will locate around both formed crystal phases. This will slow down atoms diffusion. On the other hand, new CoSi_2 nucleus is not

easy to form because Zr must be expelled from the nucleation area. The transformation of CoSi to CoSi₂ is controlled by nucleation and diffusion [12]. So CoSi and CoSi₂ in the Zr-containing thin film can keep stable until 750°C. When the thin film is annealed above 750°C, ZrSi₂ appear at grain boundaries, which supply the sites of CoSi₂ heterogeneity nucleation. At the same time, the ZrSi₂ have different lattice type and constants from CoSi and CoSi₂, so a diffusion channel around them can be set up to improve the diffusion. Then complete transformation into CoSi₂ occurred at 850°C for the Zr-containing film, as compared to 950°C for the film without Zr. However, at a lower temperature such as 750°C, although ZrSi₂ has formed, the transformation rate of CoSi is still very low. This is because a part of Zr atoms still locate at grain boundaries and the diffusion is not high enough.

Generally, polycrystalline CoSi₂ thin films suffer from a poor thermal stability and are limited to be widely used. The thermal instability of the thin films is caused by two ways [13]. Firstly, the local energy equilibrium in an as-grown thin film has not been reached at the GB triple joints on both sides of the silicide films. When the thin film is annealed at a high temperature, adjacent grains with similar energies will groove at the GB triple joints in order to reach an equilibrium state by boundary diffusion and surface diffusion. Secondly, the as-grown thin film has a high density of grain boundaries. Grains with different energies will grow to cause agglomeration when the thin film is annealed at a high temperature. Corresponding to the reasons of thermal instability, some ways that restrain the boundary and surface diffusion and grain growth will increase the thermal stability of the thin films. Tung [14] reported that Ti capping increased the uniformity and thermal stability of CoSi₂ thin film. This was attributed to two reasons. The first is the retardation of the grain boundary diffusion of CoSi₂ by Ti location at grain boundary. The second is the retardation of surface diffusion because of Ti capping. Oxygen annealing ambient [15] can also increase the thermal stability of CoSi₂ thin films, which is attributed to the formation of SiO₂ thin film and the reduction of surface diffusion. From the origination reasons of thermal instability and the ways to increase the thermal stability, we can expect the thermal stability of CoSi₂ thin film be increased by Zr addition. Zr location at the boundaries will close down the fast diffusion path at the boundaries and ZrSi₂ will slow down the grain growth. Therefore the thermal stability of CoSi₂ thin film will be increased.

Electrical resistivity of the CoSi₂ thin film is the most important property and the effect of Zr addition on it must be considered. When the thin film was annealed at a high temperature, most of Zr transformed into ZrSi₂ with a resistivity of 30–40 μΩcm, which distributed randomly in the CoSi₂ matrix. The contribution of ZrSi₂ on the electrical resistivity can be described as

$$\sigma = \sigma_0 \left(1 + \frac{c}{\frac{1-c}{3} + \frac{\sigma_0}{\sigma_1 + \sigma_0}} \right)$$

Where σ , σ_0 and σ_1 are the conductivity of the thin film, CoSi₂ and ZrSi₂, respectively. C is the volume fraction of ZrSi₂. Because the C is small and σ_1 is similar to σ_0 , we can draw the conclusion that the contribution of ZrSi₂ on the resistivity of the thin film is small. The resistivity of the Zr-contained thin film was determined as 29 μΩcm, which is a little higher than that of CoSi₂ thin film, about 20 μΩcm.

5. Conclusions

The effect of Zr addition on the formation of CoSi₂ was investigated in the paper. For the amorphous Co_{0.33}Si_{0.67} film, the crystallization activation energies of CoSi and CoSi₂ were 179.2 kJ/mol and 209.5 kJ/mol, respectively. CoSi and CoSi₂ formed in sequence. For the amorphous Co_{31.7}Si_{63.3}Zr₅ film, the crystallization activation energy of the amorphous Co_{31.7}Si_{63.3}Zr₅ film was 353.7 kJ/mol and both silicides formed simultaneously. CoSi in the Zr-containing film kept stable until 750°C while it in the thin film without Zr kept stable under 550°C. However, complete transformation into CoSi₂ occurred at 850°C for the Zr-containing film, as compared to 950°C for the film without both Zr.

Acknowledgements

The work was supported by National Natural Science Foundation of China (No. 50131030) and Shanghai AM Fundation (No. 0211)

References

1. S. P. MURARKA, *Intermetallics*, **3** (1995) 173.
2. R. T. TUNG, J. C. BEAN, J. M. GIBDOM, J. M. POATE and D. C. JACOBSON, *Appl. Phys. Lett.* **40** (1982) 684.
3. M. L. A. DASS, D. B. FRASER and C. -B. WEI, *ibid.* **58** (1991) 1308.
4. Q. Z. HONG, K. BARMACK, and L. A. CLEVINGER, *J. Appl. Phys.* **72** (1992) 3423.
5. J. Y. SHIM, S. W. PARK and H. K. BAIK, *Thin Solid Films* **292** (1997) 31.
6. A. CROS, K. N. TU, D. A. SMITH and B. Z. WEISS, *Appl. Phys. Lett.* **52** (1986) 1311.
7. F. CHENG, C. JIANG and J. WU, *Mater. Trans.* **45** (2004) 2471.
8. C. DETAVERNIER, R. L. VAN MEIRHAEGHE, F. CARDON and K. MAEX, *Phys. Rev. B* **62** (2000) 12045.
9. C. LAVOIE, C. CABRAL, JR., F. M. D'HEURLE, J. L. JORDAN-SWEET, and J. M. E. HARPER, *J. Electro. Mater.* **31** (2002) 597.
10. C. DETAVERNIER, R. L. VAN MEIRHAEGHE, F. CARDON, K. MAEX, W. VANDERVORST and B. BRIJS, *Appl. Phys. Lett.* **77** (2000) 3170.
11. B. D. CULLITY, in "Elements of X-Ray Diffraction" (Addison-Wesley Publishing Company, Inc., 1978) p. 411.
12. A. APPELBAUM, R. V. KNOELL and S. P. MURARKA, *J. Appl. Phys.* **57** (1984) 1880.
13. S. L. HSIA, T. Y. YAN, P. SMITH and G. E. MCGUIRE, *ibid.* **72** (1992) 1864.
14. R. T. TUNG and F. SCHREY, *Appl. Phys. Lett.* **67** (1995) 2164.
15. R. T. TUNG, *ibid.* **72** (1998) 2538.

Received 7 December 2004
and accepted 4 April 2005